

## Structural and computational studies of 2,5-diarylpena-2,4-dienenitriles

A. Manimekalai\*, A. Balamurugan

Department of Chemistry, Annamalai University, Annamalainagar, Tamilnadu 608 002, India

### ARTICLE INFO

#### Article history:

Received 16 January 2011

Received in revised form 27 March 2011

Accepted 28 March 2011

Available online 1 April 2011

#### Keywords:

2,5-Diarylpena-2,4-dienenitriles

Theoretical

Spectral studies

### ABSTRACT

2,5-Diarylpena-2,4-dienenitriles **1–9** were synthesized and characterized by the high resolution  $^1\text{H}$ ,  $^{13}\text{C}$ ,  $^1\text{H}-^1\text{H}$  COSY and  $^1\text{H}-^{13}\text{C}$  COSY spectra. Spectral data indicate the *trans* arrangement of the side chain protons H(3), H(4) and H(5) and *trans* orientation of H(3) proton with respect to cyano group in **1–9**. Computational calculations were carried out for some possible structures and they support the conformation in which all side chain protons are *trans* to each other and H(3) proton is *trans* to CN group. Moreover, *syn* orientation of  $\text{NO}_2$  group with respect to H(5) proton in **4–6** is revealed by computational calculations and chemical shift data. From the favored conformations, geometrical parameters, HOMO–LUMO energies, dipole moment, polarizabilities and first order hyperpolarizabilities were determined theoretically. The highest  $\beta_{\text{tot}}$  is observed for the nitrile **9** where electron releasing substituent ( $\text{OCH}_3$ ) and electron withdrawing substituent ( $\text{NO}_2$ ) are present at the opposite ends of the conjugated system and hence it is the best NLO candidate. The NLO character decreases according to the order **9 > 3 > 5 > 4 > 7 > 8 > 6 > 2 > 1**. The  $^1\text{H}$  and  $^{13}\text{C}$  chemical shifts in gaseous state as well as in solution were also determined theoretically by DFT method and they are in agreement with the experimental values. NBO analyses were further carried out for the minimum energy conformer. From  $^1\text{H}$  and  $^{13}\text{C}$  chemical shifts, the effect of introduction of substituents ( $\text{NO}_2$ ,  $\text{OCH}_3$ , Cl) in the phenyl ring on the chemical shifts of the side chain protons [H(3), H(4) and H(5)] and carbons [C(3), C(4) and C(5)] were analyzed in detail.

© 2011 Elsevier B.V. All rights reserved.

## 1. Introduction

Organic molecules with conjugated  $\pi$ -electron system are known to exhibit extremely large optical non-linear responses in terms of their molecular hyperpolarizabilities with application in many current areas of interest, such as second harmonic generation (SHG) and linear electro-optimization (LEO) [1–3]. Both theoretical and experimental studies have shown that large hyperpolarizabilities generally arise from a combination of a strong electron donor and acceptor positioned at opposite ends of a suitable conjugation path. The values obtained are dependent not only on the strength of the donor and acceptor group but also on the path length between them. Large molecular hyperpolarizability  $\beta$  arises due to the delocalization of  $\pi$ -electronic clouds [4–7]. In order to enhance the intermolecular charge transfer, most of the molecules developed as NLO materials are equipped with apparent donor and/or acceptor substituents such as nitro-, amino-, azo-, halo-, cyano-, and hydroxyl. Unsaturated nitriles play important role in biological system [8–11] and serve as versatile intermediates in the synthesis of a variety of products [12–14]. Recently they were used in the field of organic materials in order to obtain high-electron affinity polymers, which can be used to produce light

emitting diodes (LEDs) with air stable electrodes [15–17]. Synthesis, characterization and photophysical properties of novel triphenylamine derivatives containing  $\alpha,\beta$ -diarylacrylonitriles were studied in detail by Yue et al. [18]. They are found to be efficient green emitters at room temperature in solution and in solid state. Considerable work has been carried out on the synthesis and biological aspects of arylacrylonitriles derived from several substituted aromatic, heteroaromatic and aliphatic carbonyl compounds [8–11,19]. The present investigation focuses on the synthesis and theoretical investigation of the molecular structures and their NBO analysis of arylacrylonitriles with extended conjugation i.e., heavily substituted 2,5-diarylpena-2,4-dienenitriles derived from several cinnamaldehydes and arylacetonitriles and their stereochemical investigation through NMR studies. HOMO–LUMO energies, dipole moment, polarizability and first hyperpolarizabilities were determined by DFT method and compared. The  $^1\text{H}$  and  $^{13}\text{C}$  chemical shifts were also determined theoretically and compared with the observed values.

## 2. Experimental

### 2.1. Preparation of 2,5-diarylpena-2,4-dienenitriles **1–9**

To a mixture of appropriate cinnamaldehyde (0.01 mol) and potassium hydroxide (0.01 mol) in 50 mL ethanol, appropriate aryl

\* Corresponding author. Tel.: +91 9486283468.

E-mail address: [profmeka1@gmail.com](mailto:profmeka1@gmail.com) (A. Manimekalai).

acetonitrile (0.01 mol) was added and the solution was stirred for 5 min at room temperature. The solid obtained was separated, dried, and then recrystallized from absolute ethanol. The physical and mass spectral data of all the synthesized compounds are displayed in Table 1.

## 2.2. Spectral measurements

Mass spectra were recorded on VARIAN Saturn 2200 mass spectrometer with a sensitivity of 0.3 ng at 70 eV with a direct inlet system and the inlet temperature was maintained at 70 °C. Proton spectra at 500 MHz and proton decoupled  $^{13}\text{C}$  NMR spectra at 125 MHz were recorded at room temperature on DRX 500 NMR spectrometer using 10 mm sample tubes. Samples were prepared by dissolving about 10 mg of the sample in 0.5 mL of chloroform-*d* containing 1% TMS for  $^1\text{H}$  and 0.5 g of the sample in 2.5 mL of chloroform-*d* containing a few drops of TMS for  $^{13}\text{C}$ . The solvent chloroform-*d* also provided the internal field frequency lock signal. Proton spectrum has the following experimental parameters: number of scans 32; spectral width 6009 Hz; acquisition time 2.73 s. The experimental parameters for  $^{13}\text{C}$  NMR spectra are: spectral width 32,768 Hz; number of scans ranges from 64 to 468; acquisition time 1.20 s.

The  $^1\text{H}$ - $^1\text{H}$  COSY spectra were performed on a DRX-500 NMR spectrometer at 500 MHz using the standard pulse sequences employing the TPPI method to obtain pure absorption mode spectra. For  $^1\text{H}$ - $^1\text{H}$  COSY spectra the experimental parameters are: number of scans 16, acquisition time 0.15 s, spectral width 6666 Hz.  $^1\text{H}$ - $^{13}\text{C}$  COSY spectra were obtained on a DRX-500 NMR spectrometer using standard parameters: the number of scans 16; number of data points 2048; acquisition time 0.15 s and spectral width 6666 Hz.

## 2.3. Computational study

Geometry optimizations were carried out according to Density Functional Theory available in Dmol<sup>3</sup> [hybrid functional BLYP with the basis set dnp] [20] and Gaussian-03 package [B3LYP/6-31G(d,p) basis set] [21] for all the structures of nitriles **1–9**. The electric dipole moment, polarizabilities and hyperpolarizabilities were determined from the DFT optimized structures by finite field

approach using B3LYP/6-31G\* basis set available in Gaussian-03 package. The  $^1\text{H}$  and  $^{13}\text{C}$  chemical shifts were determined theoretically by DFT method in gaseous state as well as in  $\text{CDCl}_3$  [SCRF-PCM model] using the basis set B3LYP/6-311+G(2d,p) Gao. NBO calculations were determined theoretically by DFT method using the basis set B3LYP/6-31G(d) and B3LYP/6-311+G(d,p).

## 3. Results and discussion

2,5-Diphenylpenta-2,4-dienenitrile (**1**), 2-(*p*-chlorophenyl)-5-phenylpenta-2,4-dienenitrile (**2**), 2-(*p*-nitrophenyl)-5-phenylpenta-2,4-dienenitrile (**3**), 5-(*o*-nitrophenyl)-2-phenylpenta-2,4-dienenitrile (**4**), 2-(*p*-chlorophenyl)-5-(*o*-nitrophenyl)penta-2,4-dienenitrile (**5**), 2-(*p*-nitrophenyl)-5-(*o*-nitrophenyl)penta-2,4-dienenitrile (**6**), 5-(*p*-methoxyphenyl)-2-phenylpenta-2,4-dienenitrile (**7**), 2-(*p*-chlorophenyl)-5-(*p*-methoxyphenyl)penta-2,4-dienenitrile (**8**) and 2-(*p*-nitrophenyl)-5-(*p*-methoxyphenyl)penta-2,4-dienenitrile (**9**) were synthesized according to the Scheme 1 and the high resolution  $^1\text{H}$ ,  $^{13}\text{C}$ ,  $^1\text{H}$ - $^1\text{H}$  COSY and  $^1\text{H}$ - $^{13}\text{C}$  COSY NMR spectra have been recorded in  $\text{CDCl}_3$  and analyzed. The  $^1\text{H}$  and  $^{13}\text{C}$  NMR spectra reveal the presence of only one isomer in solution. The signals in the  $^1\text{H}$  NMR spectra were assigned based on their positions, integrals and multiplicities and confirmed by the correlations observed in the COSY spectra. In  $^{13}\text{C}$  NMR spectra quaternary carbon can be easily distinguished from other carbons based on small intensities. Assignments of the aromatic ring carbons and side chain carbons made on the basis of cross peaks observed in  $^1\text{H}$ - $^{13}\text{C}$  COSY spectra. For example the assignments of signals in the nitrile **1** are made as follows.

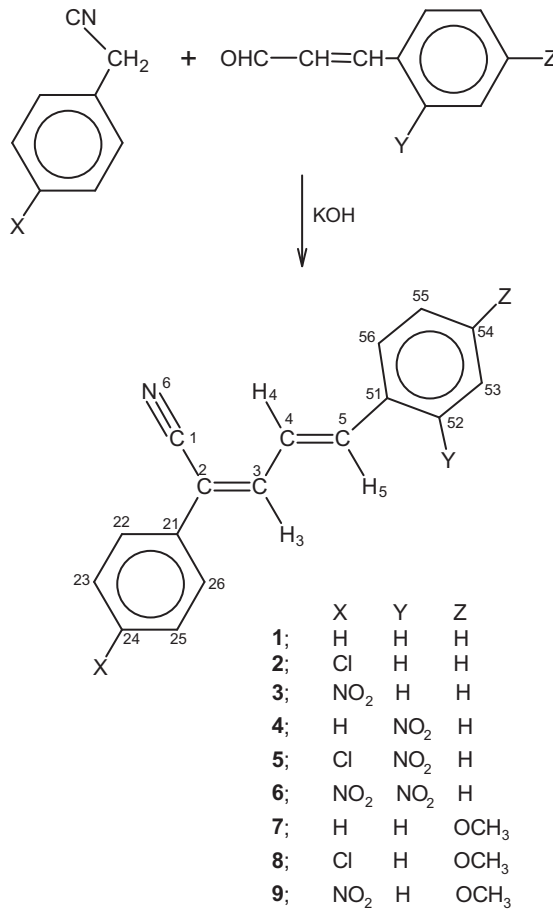


**Table 1**  
Physical and mass spectral data of **1–9**.

Compounds	Physical data		Mass spectral data ( <i>m/z</i> )
	Colour	Yield (%)	
<b>1</b>	Greenish yellow	84	167–168, 231.9 [M+1], 231.0 [M] <sup>+</sup> , 230.1, 152.9, 91.0, 51.1
<b>2</b>	Greenish yellow	82	144–145, 267.9 [M+2], 266.0 [M] <sup>+</sup> , 266.8 [M+1], 265.1, 231.2, 230.2, 115.1, 51.1
<b>3</b>	Greenish yellow	82	142–143, 278 [M+2], 277 [M+1], 247.1, 132.1, 115.0
<b>4</b>	Green	78	176–177, 275.8 [M] <sup>+</sup> , 275.0 [M–1], 247.1, 242.2, 222.2, 204.1, 156.0, 132.0, 119.0, 117.4, 115.2, 92.0, 83.0
<b>5</b>	Green	77	200–201, 309.7 [M] <sup>+</sup> , 308.9, 292.8, 258.1, 257.2, 131.9, 119.8, 92.0, 75.8
<b>6</b>	Green	78	104–105, 323.2, 322.0 [M+2], 319.6 [M] <sup>+</sup> , 105.1, 77.0, 51.0
<b>7</b>	Greenish yellow	85	144–145, 262.1 [M+1], 261.0 [M] <sup>+</sup> , 246.3, 184.1, 121.2, 51.0
<b>8</b>	Greenish yellow	84	167–168, 298.0, 296.0 [M+1], 295.1 [M] <sup>+</sup> , 260.3, 245.2, 144.8, 50.1
<b>9</b>	Greenish yellow	84	144–145, 308.0 [M+2], 307.0 [M+1], 306.0 [M] <sup>+</sup> , 54.9

**Scheme 1.** Structures of **1–9**.

<sup>13</sup>C NMR spectrum of **1** shows signals at 141.58, 141.23, 135.79, 133.28, 129.55, 129.07, 128.94, 127.53, 125.63, 125.19, 116.95 and 113.22 ppm. Based on small intensities the signals at 135.79, 133.28, 116.95 and 113.22 ppm are assigned to the quaternary carbons. Among quaternary carbon signals, the signals at 135.79 and 133.28 ppm should be due to *ipso* carbons of phenyl ring. The remaining signals at 113.22 and 116.95 ppm are due to carbon possessing cyano group (CCN) and cyano carbon (CN) respectively and this assignments is based on the expectation that the cyano bearing carbon resonates at lower frequency compared to cyano carbon [22]. From the comparison of chemical shifts of the *ipso* carbons in nitrile **1** (135.79 and 133.28 ppm) with those nitriles **2** and **3**. It is concluded that the signal at 135.79 ppm is due to *ipso* carbon of phenyl ring at C5 (C51). Obviously the remaining signal at 133.28 ppm is due to *ipso* carbon of phenyl ring at C2 (C21). The remaining signals are assigned based on the correlations observed

in <sup>1</sup>H–<sup>13</sup>C COSY spectrum. In a similar manner assignments were done for **2–9**. The various chemical shifts and coupling constants determined in this manner for **1–9** are reported in the Tables 2 and 3.

### 3.1. Conformation of 2,5-diarylpena-2,4-dienenitriles

#### 3.1.1. Spectral studies

It is seen from Table 2 that the two couplings associated with H(4) signal in **4–9** are in the range 11 and 15 Hz ( $J_{3,4}$  and  $J_{4,5}$ ). The large magnitude suggest that the two nearby protons H(3) and H(5) must be *trans* to the side chain proton H(4). There are two possible ways of attaching the cyano and aryl groups at C-2, (i) cyano group is *anti* to H(3) [**A**] i.e., **Z** configuration and (ii) cyano group is *syn* to H(3) [**B**] i.e., **E** configuration as shown in Scheme 2. Previously it has been established that in 3-aryl-2-phenylacrylo-

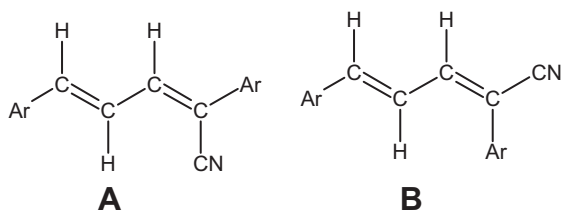
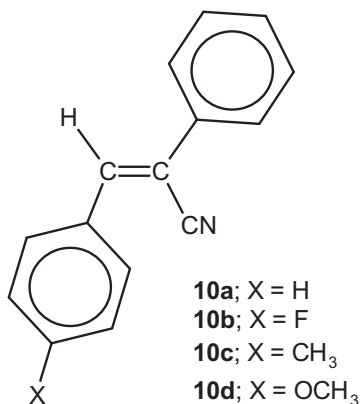
**Table 2**  
<sup>1</sup>H chemical shifts (ppm) of **1–9**.

Compounds	H(3)	H(4)	H(5)	Aromatic protons C(2)	C(5)
<b>1</b>	7.45–7.35	7.45–7.35	7.03 [dd, 2.91 ( $J_{3,5}$ ), 11.54 ( $J_{4,5}$ ) Hz]	7.64 (d, 7.46 Hz) [H(22), H(26)] 7.45–7.35 [H(23), H(24), H(25)]	7.56 (d, 7.05 Hz) [H(52), H(56)] 7.45–7.35 [H(53), H(54), H(55)]
<b>2</b>	7.40–7.33	7.40–7.33	7.03 [dd, 3.17 ( $J_{3,5}$ ), 11.14 ( $J_{4,5}$ ) Hz]	7.54 (d, 8.41 Hz) [H(22), H(26)] 7.33–7.40 [H(23), H(25)]	7.54 (d, 8.41 Hz) [H(52), H(56)] 7.33–7.40 [H(53), H(54), H(55)]
<b>3</b>	7.63–7.55	7.45–7.40	7.16 [dd, 4.50 ( $J_{3,5}$ ), 15.25 ( $J_{4,5}$ ) Hz]	7.79 (d, 8.95 Hz) [H(22), H(26)] 8.29 (d, 8.90 Hz) [H(23), H(25)]	7.63–7.55 [H(52), H(56)] 7.45–7.40 [H(53), H(54), H(55)]
<b>4</b>	7.48 [d, 11.30 ( $J_{3,4}$ ) Hz]	7.37 [dd, 15.23 ( $J_{4,5}$ ), 11.18 ( $J_{3,4}$ ) Hz]	7.55 [d, 15.15 ( $J_{4,5}$ ) Hz]	7.65–7.68 [H(22), H(26)] 7.41–7.51 [H(23), H(24), H(25)]	8.01 (dd, 8.20, 1.05 Hz) [H(53)] 7.41–7.51 [H(54)] 7.65–7.68 [H(55)] 7.83 (d, 7.40 Hz) [H(56)]
<b>5</b>	7.46 [d, 11.20 ( $J_{3,4}$ ) Hz]	7.35 [dd, 15.13 ( $J_{4,5}$ ), 11.13 ( $J_{3,4}$ ) Hz]	7.57 [d, 14.95 ( $J_{4,5}$ ) Hz]	7.59 (d, 8.55 Hz) [H(22), H(26)] 7.42 (d, 8.60 Hz) [H(23), H(25)]	8.02 (d, 8.15 Hz) [H(53)] 7.51 [H(54)], 7.67 [H(55)] 7.83 (d, 7.75 Hz) [H(56)]
<b>6</b>	7.64 [d, 11.10 ( $J_{3,4}$ ) Hz]	7.39 [dd, 15.20 ( $J_{4,5}$ ), 11.20 ( $J_{3,4}$ ) Hz]	7.71 [d, 15.15 ( $J_{4,5}$ ) Hz]	7.838 (d, 8.80 Hz) [H(22), H(26)] 8.32 (d, 8.80 Hz) [H(23), H(25)]	8.07 (d, 8.20 Hz) [H(53)] 7.56 [H(54)], 7.73 [H(55)] 7.844 (d, 7.33 Hz) [H(56)]
<b>7</b>	7.39 [d, 11.25 ( $J_{3,4}$ ) Hz]	7.27 [dd, 15.23 ( $J_{4,5}$ ), 11.23 ( $J_{3,4}$ ) Hz]	6.97 [d, 15.20 ( $J_{4,5}$ ) Hz]	7.61 (d, 7.60 Hz) [H(22), H(26)] 7.41 [H(23), H(25)] 7.34 [H(24)]	≈7.50 [H(52), H(56)] ≈6.91 [H(53), H(55)]
<b>8</b>	7.35 [d, 10.80 ( $J_{3,4}$ ) Hz]	7.23 [dd, 15.18 ( $J_{4,5}$ ), 11.23 ( $J_{3,4}$ ) Hz]	6.97 [d, 15.15 ( $J_{4,5}$ ) Hz]	7.52 (d, 8.60 Hz) [H(22), H(26)] 7.36 (d, 8.40 Hz) [H(23), H(25)]	7.49 (d, 8.70 Hz) [H(52), H(56)] 6.91 (d, 8.70 Hz) [H(53), H(55)]
<b>9</b>	7.55 [d, 11.20 ( $J_{3,4}$ ) Hz]	7.29 [dd, 15.30 ( $J_{4,5}$ ), 11.30 ( $J_{3,4}$ ) Hz]	7.12 [d, 15.25 ( $J_{4,5}$ ) Hz]	7.76 (d, 8.90 Hz) [H(22), H(26)] 8.27 (d, 8.90 Hz) [H(23), H(25)]	7.54 (d, 8.65 Hz) [H(52), H(56)] 6.94 (d, 8.75 Hz) [H(53), H(55)]

Values within parentheses are observed coupling constants derived from the particular signal.

**Table 3**  
<sup>13</sup>C chemical shifts (ppm) of **1–9**.

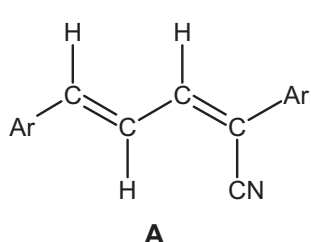
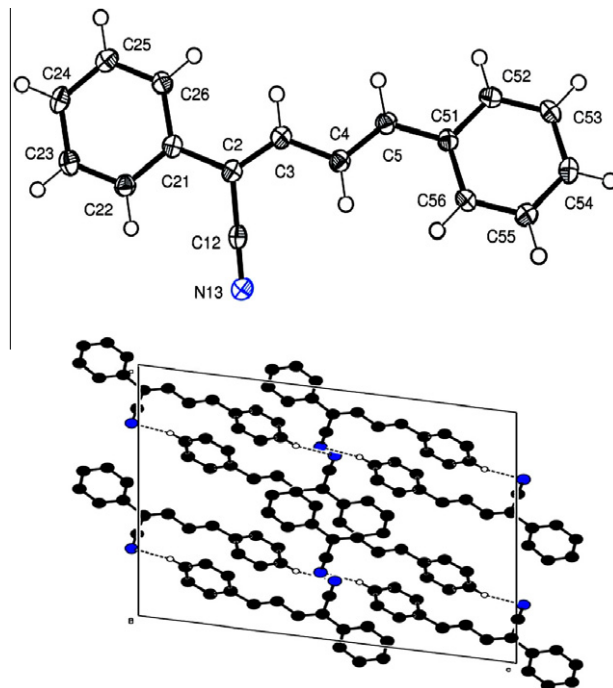
Compounds	C(3)	C(4)	C(5)	CCN	CN	<i>ipso</i> carbons	Other carbons	
							C(2) aromatic	C(5) aromatic
<b>1</b>	141.58	125.19	141.23	113.22	116.95	135.79 [C(51)] 133.28 [C(21)]	125.63 [C(22), C(26)] 129.07 [C(23), C(24), C(25)]	127.53 [C(52), C(56)] 128.94 [C(53), C(55)] 129.55 [C(54)]
<b>2</b>	141.90	124.87	141.85	111.86	116.62	135.56 [C(51)] 131.73 [C(21)] 135.01 [C(24)]	126.75 [C(22), C(26)] 129.24 [C(23), C(25)]	127.57 [C(52), C(56)] 128.93 [C(53), C(55)] 129.71 [C(54)]
<b>3</b>	145.04	124.63	144.41	110.86	116.09	135.24 [C(51)] 139.44 [C(21)] 147.68 [C(24)]	126.20 [C(22), C(26)] 124.40 [C(23), C(25)]	127.96 [C(52), C(56)] 129.10 [C(53), C(55)] 130.42 [C(54)]
<b>4</b>	140.45	129.73	135.08	115.92	116.51	131.29 [C(51)] 132.67 [C(21)] 148.05 [C(52)]	125.86 [C(22), C(26)] 129.16 [C(23), C(25)] 129.62 [C(24)]	125.03 [C(53)] 129.55 [C(54)] 133.41 [C(55)] 128.49 [C(56)]
<b>5</b>	140.81	129.42	135.73	111.24	116.21	131.22 [C(51), C(24)] 131.22 [C(21)] 148.07 [C(52)]	127.07 [C(22), C(26)] 129.72 [C(23), C(25)]	125.08 [C(53)] 129.72 [C(54)] 133.47 [C(55)] 128.53 [C(56)]
<b>6</b>	143.98	128.90	138.25	113.56	115.66	131.59 [C(51)] 148.13 [C(24)] 148.13 [C(52)] 138.74 [C(21)]	126.58 [C(22), C(26)] 124.43 [C(23), C(25)]	125.16 [C(53)] 130.24 [C(54)] 133.60 [C(55)] 128.67 [C(56)]
<b>7</b>	142.08	123.15	141.00	111.65	117.23	133.47 [C(21)] 128.61 [C(51)] 160.88 [C(54)]	125.46 [C(22), C(26)] 129.01 [C(23), C(25)] 128.79 [C(24)]	129.09 [C(52), C(56)] 114.42 [C(53), C(55)] 55.38 [OCH <sub>3</sub> ]
<b>8</b>	142.39	122.87	141.62	110.33	116.90	131.99 [C(21)] 134.65 [C(24)] 161.01 [C(54)] 128.43 [C(51)]	126.60 [C(22), C(26)] 129.19 [C(23), C(25)]	129.19 [C(52), C(56)] 114.44 [C(53), C(55)] 55.37 [OCH <sub>3</sub> ]
<b>9</b>	145.52	122.56	144.29	109.16	116.43	139.70 [C(21)] 147.33 [C(24)] 128.07 [C(51)] 161.56 [C(54)]	125.91 [C(22), C(26)] 124.33 [C(23), C(25)]	129.67 [C(52), C(56)] 114.58 [C(53), C(55)] 55.48 [OCH <sub>3</sub> ]

**Scheme 2.** Possible configurations of cyano group.**Fig. 1.** Structure of nitrile **10**.

nitriles (**10a–10d**) (Fig. 1), the two aryl rings are occupying *trans* arrangement and the side chain CH protons resonate in the region 7.40–7.54 ppm [22–24]. The chemical shifts of H(3) in the nitriles **4–9** are closer to the values reported in **10a–10d** and hence in **4–9** also H(3) protons must be *trans* to CN group. The chemical shifts of H(3) in **1–3** are closer to **4–9** and hence one can expect that H(3) protons must be *trans* to CN group in **1–3** also. Therefore, the favored structures of 2,5-diarylpenta-2,4-dienenitriles **1–9** are predicted to be **A** in which all the side chain protons are *trans* to each other and H(3) protons are *trans* to CN group (Fig. 2). For **1** single crystal measurements were also made [25] and it reveals the geometry **A** in which all the side chain protons are *trans* to each other. The molecule belongs to the monoclinic crystal lattice (*C*2/c). The ORTEP and the close packed structures are given in Fig. 3.

#### Crystal data

$\text{C}_{17}\text{H}_{13}\text{N}$	$V = 2456.42(13)\text{\AA}^3$
$M_r = 231.28$	$Z = 8$
Monoclinic, <i>C</i> 2/c	Cu K $\alpha$ radiation
$a = 16.9390(5)\text{\AA}$	$\mu = 0.56\text{ mm}^{-1}$
$b = 7.5869(2)\text{\AA}$	$T = 110\text{ K}$
$c = 19.3809(6)\text{\AA}$	$0.53 \times 0.36 \times 0.29\text{ mm}$
$\beta = 92.521(3)^\circ$	

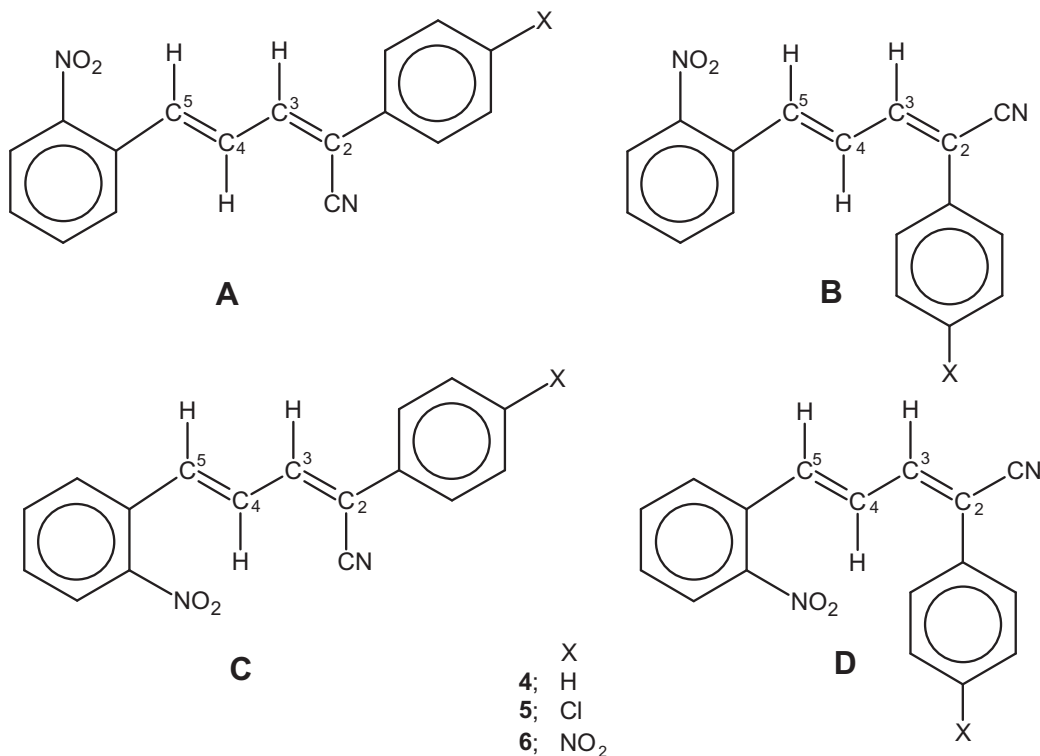
**Fig. 2.** Favored conformations of **1–9**.**Fig. 3.** ORTEP and close packed structures of **1**.

#### 3.1.2. Theoretical studies

In order to predict the favored conformation of penta-2,4-dienenitriles **1–9** in gaseous state, theoretical studies were also performed in the present study. Since *trans*-cinnamaldehyde was used as one of the starting materials for the synthesis of nitriles all the side chain protons must be *trans* to each other in **1–9** and only two isomers possible for the nitriles **1–3** and **7–9** as shown in Scheme 2. In the isomer **A** the cyano group is *anti* to H(3) whereas in **B** it is *syn* to H(3). For the nitrile derivatives derived from *o*-nitrocinnamaldehyde i.e., **4–6** there are two more structures as shown in Scheme 3 are possible. In isomers **A** and **B** the nitro group adopts *syn* orientation with respect to H(5) proton whereas in structures **C** and **D** the nitro group adopts *anti* orientation with respect to H(5). In structures **A** and **C**, cyano group is *anti* to H(3) whereas in structures **B** and **D** the cyano group is *syn* to H(3).

Computational calculations were carried out according to Density Functional Theory available in Dmol<sup>3</sup> and Gaussian-03 package for all the structures shown in Schemes 2 and 3. Table 4 reports the energies of nitriles **1–9** according to these methods. Calculations reveal that **Z** isomer [**A**] is thermodynamically favored over the **E** isomer [**B**] in all the nitriles and nitro group prefers *syn* orientation with respect to H(5) in nitriles **4–6**. The spectral studies also predict the same geometries. Thus, the geometries predicted in solution (NMR study) are in agreement with the geometries predicted in the gaseous state.

The DFT [B3LYP/6-31G(d,p)] optimized structures of **1–9** are reproduced in Fig. 4. The geometric parameters derived from the favored conformations according to Dmol<sup>3</sup> and Gaussian methods are reported in Table 5. In most of the cases there is a good agreement between the values. Only slight variation in the geometric parameters (bond lengths and bond angles) by varying the basis set are observed in the present study. Deviations are observed only in some torsional angles. The torsional angles C4–C5–C51–C52 and C4–C5–C51–C56 in **4–6** around 156° and 28° indicate that the *o*-nitrophenyl ring at C-5 is tilted from the plane



Scheme 3. Possible conformations of nitro group.

**Table 4**  
DFT energies of possible isomers of nitriles **1–9**.

Compounds	Isomers	Energy (hartrees)	
		Dmol <sup>3</sup>	Gaussian-03
<b>1</b>	<b>A</b>	−710.3261829	−710.3808157
	<b>B</b>	−710.3224585	−710.3769114
<b>2</b>	<b>A</b>	−1169.9556548	−1169.974859
	<b>B</b>	−1169.9516894	−1169.9708903
<b>3</b>	<b>A</b>	−914.9180623	−914.8802554
	<b>B</b>	−914.9134514	−914.8756887
<b>4</b>	<b>A</b>	−914.9093353	−914.8727347
	<b>B</b>	−914.9041518	−914.8681545
	<b>C</b>	−914.9026229	−914.8647505
	<b>D</b>	−914.9005451	−914.8643782
<b>5</b>	<b>A</b>	−1374.5371179	−1374.4664979
	<b>B</b>	−1374.5336127	−1374.4618194
	<b>C</b>	−1374.5317713	−1374.4586084
	<b>D</b>	−1374.5301577	−1374.4583501
<b>6</b>	<b>A</b>	−1119.4995644	−1119.3709499
	<b>B</b>	−1119.4945854	−1119.3660786
	<b>C</b>	−1119.4932249	−1119.3633093
	<b>D</b>	−1119.4911207	−1119.3625873
<b>7</b>	<b>A</b>	−824.8693374	−824.9074083
	<b>B</b>	−824.8656181	−824.9035803
<b>8</b>	<b>A</b>	−1284.4990757	−1284.5016459
	<b>B</b>	−1284.4951218	−1284.4977103
<b>9</b>	<b>A</b>	−1029.4622544	−1029.4075938
	<b>B</b>	−1029.4573121	−1029.4030247

the phenyl ring at C-2 also. HOMO–LUMO energies were also calculated and the values are listed in Table 6. The electric dipole moment, polarizabilities and first order polarizabilities were also calculated by DFT method using the basis set B3LYP/6-31G\* available in Gaussian-03 package and these values are listed in Tables 7 and 8.

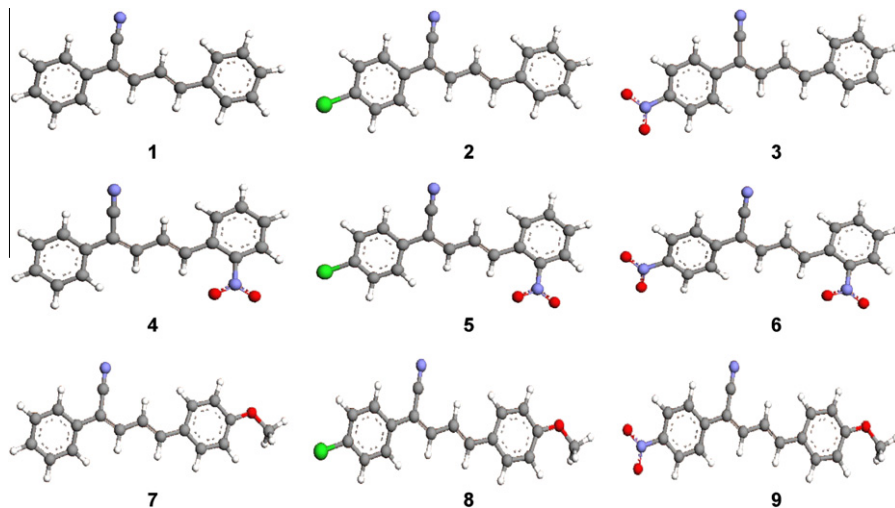
HOMO and LUMO orbitals are stabilized by the introduction of chloro and nitro substituents at the *para* position of the phenyl ring at C-2 and nitro substituent at the *ortho* position of phenyl ring at C-5 whereas electron releasing *para*-methoxy substituent at C-5 destabilizes both HOMO and LUMO orbitals. From Table 7, it is seen that the introduction of chloro and nitro substituent at the *para* position of phenyl ring at C-2 and methoxy substituent at the *para* position of phenyl ring at C-5 increases both the dipole moments and polarizabilities. However, the introduction of nitro substituent at the *ortho* position of phenyl ring at C-5 decreases dipole moment but increases polarizability values.

Second order NLO calculations and comparison of the NLO properties of various substituted systems reveal that the presence of NO<sub>2</sub> group enhances the second order NLO properties of the molecules [4–7,26,27]. Large first order hyperpolarizability is expected for the 2,5-diarylpena-2,4-dienenitriles **1–9** since extensive delocalization is present in this system. Table 8 reveals that first order hyperpolarizability is dominated by the component  $\beta_{xxx}$ . The highest  $\beta_{tot}$  is observed for the nitrile **9** where electron releasing substituent (OCH<sub>3</sub>) and electron withdrawing substituent (NO<sub>2</sub>) are present at the opposite ends of the conjugated system. Among the nitriles, the best NLO candidate is **9**. The NLO character decreases according to the following order:

$$\mathbf{9} > \mathbf{3} > \mathbf{5} > \mathbf{4} > \mathbf{7} > \mathbf{8} > \mathbf{6} > \mathbf{2} > \mathbf{1}.$$

The macroscopic susceptibility in the condensed phase assuming the electric fields to be the same is directly proportional to the microscopic (hyper) polarizabilities. The electric field experienced

containing the side chain moiety in **4–6**. This is further supported by the torsional angles H5–C5–C51–C52 ( $\approx 23^\circ$ ) and H5–C5–C51–C56 ( $\approx 152^\circ$ ). The torsional angles C22–C21–C2–C3, C22–C21–C2–C1, C26–C21–C2–C3 and C26–C21–C2–C1 indicate the tilting of

**Fig. 4.** Optimized structures of favored conformations of **1–9**.**Table 5**Selected geometric parameters [bond lengths (Å), bond angles (°) and torsional angles (°)] in **1–9**.

Geometric parameters	<b>1</b> XRD	<b>2</b> Theor.	<b>3</b>	<b>4</b>	<b>5</b>	<b>6</b>	<b>7</b>	<b>8</b>	<b>9</b>	
<i>Bond lengths</i>										
C1–C2	1.445 (1.437)	1.435 (1.436)	1.435 (1.437)	1.435 (1.437)	1.436 (1.438) 1.436 (1.438)	1.436 (1.438) (1.438)	1.435 (1.436)	1.434 (1.436) (1.436)	1.435 (1.436)	
C2–C3	1.354 (1.379)	1.368 (1.380)	1.368 (1.380)	1.370 (1.381)	1.366 (1.380) 1.367 (1.380)	1.367 (1.380) (1.380)	1.367 (1.380)	1.369 (1.381) (1.380)	1.371 (1.384)	
C3–C4	1.442 (1.431)	1.435 (1.431)	1.435 (1.431)	1.433 (1.429)	1.438 (1.432) 1.437 (1.431)	1.437 (1.431) (1.432)	1.436 (1.430)	1.434 (1.430)	1.430 (1.426)	
C4–C5	1.345 (1.366)	1.356 (1.367)	1.357 (1.368)	1.358 (1.368)	1.355 (1.367) 1.355 (1.369)	1.355 (1.369) (1.366)	1.356 (1.368)	1.358 (1.368)	1.361 (1.371)	
C5–C51	1.465 (1.458)	1.459 (1.458)	1.459 (1.458)	1.457 (1.456)	1.465 (1.460) 1.465 (1.462)	1.465 (1.462) (1.462)	1.465 (1.454)	1.454 (1.453) (1.450)	1.451 (1.450)	
C2–C21	1.484 (1.484)	1.481 (1.483)	1.480 (1.479)	1.478 (1.479)	1.480 (1.481) 1.479 (1.480)	1.479 (1.480) (1.480)	1.479 (1.484)	1.480 (1.483) (1.478)	1.477 (1.478)	
C1–N6	1.149 (1.171)	1.165 (1.171)	1.165 (1.171)	1.165 (1.171)	1.165 (1.173) 1.165 (1.171)	1.165 (1.171) (1.170)	1.164 (1.170)	1.165 (1.171)	1.165 (1.171)	
C24–Cl	— —	— (1.766)	— (1.766)	— —	— —	1.755 (1.763) —	— —	1.757 (1.757) —	— —	
C24–N	— —	— —	— —	1.468 (1.481)	— —	— —	1.469 (1.486)	— —	— —	1.466 (1.467)
C52–N	— —	— —	— —	— —	1.474 (1.490) 1.474 (1.503)	1.474 (1.503) (1.491)	— —	— —	— —	— —
C54–O	— —	— —	— —	— —	— —	— —	— —	1.360 (1.376)	1.359 (1.359) 1.357 (1.373)	
<i>Bond angles</i>										
C21–C2–C3	125.3 (125.1)	124.6 (125.0)	124.6 (124.8)	124.4 (124.8)	124.6 (125.2) 124.6 (125.2)	124.6 (125.2) (125.1)	124.5 (125.1)	124.5 (125.0) (124.4)	124.4 (124.7)	
C2–C3–C4	126.2 (126.2)	126.0 (126.5)	126.0 (126.3)	126.0 (126.3)	125.6 (125.9) 125.6 (125.7)	125.6 (125.7) (125.6)	126.2 (126.5)	126.1 (126.6) (126.0)	126.0 (126.5)	
C3–C4–C5	121.4 (122.9)	122.4 (122.4)	122.3 (122.4)	122.1 (122.4)	122.3 (122.3) 122.2 (122.1)	122.2 (122.1) (122.3)	122.0 (122.7)	122.4 (122.7)	122.3 (122.5) (122.3)	
C4–C5–C51	127.2 (127.5)	127.6 (127.9)	127.6 (127.7)	127.6 (127.7)	124.5 (125.8) 124.5 (126.0)	124.5 (126.0) (125.6)	124.5 (127.8)	127.7 (127.7) (127.8)	127.6 (127.9)	
C21–C2–C1	116.6 (117.0)	117.0 (116.9)	117.0 (116.9)	117.1 (117.1)	117.1 (117.2) 117.0 (117.0)	117.0 (117.0) (117.2)	117.0 (117.2)	117.0 (117.0) (117.0)	117.0 (117.0) (117.2)	
C3–C2–C1	118.1 (117.9)	118.4 (118.0)	118.5 (118.0)	118.5 (118.1)	118.3 (117.7) 118.4 (117.8)	118.4 (117.8) (117.8)	118.4 (117.8)	118.5 (118.0) (117.9)	118.4 (118.1)	
<i>Torsional angles</i>										
C1–C2–C3–C4	−2.7	−2.0 (−0.6)	−2.1 (−0.5)	−1.8 (−0.7)	2.3 (0.8)	2.4 (0.6)	−1.8 (0.3)	−2.1 (−0.6)	−2.1 (−0.4)	−1.8 (−0.6)
C2–C3–C4–C5	177.4	179.2 (178.3)	179.1 (178.5)	179.1 (178.4)	−178.9 (−180.0)	−179.0 (−179.6)	179.8 (180.0)	179.0 (178.2)	179.0 (179.0) (178.4)	178.9 (178.4)
C3–C4–C5–C51	177.5	−179.9 (179.9)	180.0 (−179.7)	179.9 (179.8)	177.8 (179.0)	178.0 (179.7)	177.9 (179.0)	179.9 (179.8)	−189.0 (−179.5)	180.0 (−179.9)
C4–C5–C51–C56	−15.2	0.3 (−3.3)	−0.4 (−2.7)	−0.3 (−3.4)	−27.0 (−14.7)	−27.3 (−3.6)	−27.8 (−16.1)	0.0 (−2.7)	−0.4 (−2.2)	−0.4 (−2.5)

(continued on next page)

**Table 5** (continued)

Geometric parameters	<b>1</b>	<b>2</b>	<b>3</b>	<b>4</b>	<b>5</b>	<b>6</b>	<b>7</b>	<b>8</b>	<b>9</b>	
	XRD	Theor.								
C4–C5–C51–C52	165.3	−179.7 (176.7)	179.7 (177.3)	179.8 (176.8)	156.4 (168.5)	156.0 (177.3)	155.5 (167.3)	−180.0 (177.3)	179.6 (177.8)	179.6 (177.6)
C5–C51–C52–H52	–	0.0 (−0.7)	0.0 (−0.1)	−0.0 (−0.2)	–	–	–	0.0 (−0.1)	0.0 (0.0)	0.0 (0.1)
C5–C51–C56–H56	–	0.0 (−0.4)	0.0 (−0.3)	0.0 (−0.3)	−0.1 (0.0)	−0.2 (0.4)	−0.2 (0.4)	0.0 (−0.3)	0.0 (−0.4)	−0.1 (−0.3)
C21–C2–C3–C4	177.8	179.0 (179.6)	179.0 (−179.8)	179.5 (179.7)	−179.0 (−179.7)	−178.8 (−179.5)	179.7 (179.3)	179.0 (179.9)	179.0 (−179.8)	179.4 (180.0)
C22–C21–C2–C3	−176.4	179.0 (178.5)	160.3 (179.3)	162.3 (178.3)	−159.5 (−178.7)	160.6 (−179.8)	163.8 (177.3)	159.5 (178.8)	−160.4 (179.7)	163.2 (179.0)
C22–C21–C2–C1	4.1	−19.6 (−1.4)	−18.6 (0.0)	−16.4 (−1.3)	19.2 (0.9)	18.1 (0.2)	−15.4 (−2.3)	−19.5 (−0.7)	−18.5 (0.4)	−15.6 (−0.4)
C26–C21–C2–C1		160.3 (178.5)	161.3 (179.8)	163.5 (178.7)	−160.8 (−179.3)	160.8 (−179.5)	164.4 (177.9)	160.5 (179.2)	161.4 (179.4)	164.3 (179.8)
C26–C21–C2–C3	3.3	−20.7 (−1.7)	−19.7 (−0.4)	−17.8 (−1.7)	20.4 (1.1)	19.4 (0.5)	−16.4 (−2.5)	−20.6 (−1.2)	−19.7 (−0.1)	−17.0 (−0.8)
H26–C26–C21–C2	–	−2.9 (0.0)	−2.8 (−0.2)	−2.7 (−0.1)	2.9 (0.0)	2.8 (−0.1)	−2.4 (−0.9)	−2.8 (0.0)	−2.8 (−0.2)	−2.6 (−0.2)
C5–C51–C52–N	–	–	–	–	−4.7 (−4.1)	−4.7 (−1.7)	4.7 (−4.7)	–	–	–
H22–C22–C21–C2	–	0.7 (0.0)	0.73 (0.3)	0.7 (0.1)	−0.8 (−0.3)	−0.7 (0.5)	0.5 (0.3)	0.7 (−0.1)	0.7 (0.4)	0.6 (0.2)
H3–C3–C4–H4	–	−179.9 (178.9)	−179.9 (179.3)	−179.8 (178.9)	−178.3 (−178.5)	−178.2 (−179.3)	−177.6 (178.0)	−180.0 (179.1)	−180.0 (179.5)	−179.9 (179.2)
H4–C4–C5–H5	–	−179.9 (179.1)	179.9 (179.2)	179.9 (179.0)	175.5 (176.5)	175.6 (179.0)	175.7 (176.5)	180.0 (179.0)	179.9 (179.2)	179.9 (179.0)
H3–C3–C4–C5	–	0.1 (−1.6)	0.0 (−1.3)	0.1 (−1.5)	0.2 (0.2)	0.2 (0.4)	0.8 (0.5)	0.0 (−1.5)	−0.1 (−1.2)	0.0 (−1.3)
H4–C4–C5–C51	–	0.0 (−0.5)	−0.1 (−0.2)	−0.1 (−0.6)	−3.7 (−2.4)	−3.6 (−0.6)	−3.8 (−2.6)	0.0 (−0.4)	−0.1 (−0.2)	−0.1 (−0.5)
H5–C5–C51–C56	–	−179.7 (177.1)	179.6 (177.8)	179.7 (177.0)	153.7 (166.4)	153.4 (176.8)	152.7 (164.9)	−180.0 (177.8)	179.6 (178.4)	179.6 (178.0)
H5–C5–C51–C52	–	0.3 (−2.9)	−0.3 (−2.2)	−0.3 (−2.9)	−22.8	−23.2 (−2.4)	−23.9 (−10.4)	0.0 (−2.2)	−0.4 (−1.7)	−0.4 (−1.9)

Values within parentheses are calculated values according to the Dmol<sup>3</sup> structures.

by the individual molecules in a macroscopic sample is not the same as the applied external electric field which would be experienced by an isolated molecule in the gas phase. Instead the molecule in a macroscopically applied field experiences a local field  $E_{loc}^w$  [28]. This field (not known) is different from the macroscopically applied field (used in experiment is well known) because of

polarization of surrounding molecules. Therefore, non-linear optical properties of a molecule in solution or in solid state will be different from that of isolated molecule due to polarization effects caused by the surrounding molecules. Even though theoretical studies can be performed in liquid phase it does not solve the issue of local field effects. The hyperpolarizability  $\beta$  in solution can be theoretically

**Table 6**  
Calculated HOMO–LUMO energies (eV) of nitriles **1–9**.

Compounds	LUMO		HOMO		Energy gap ( $\Delta E$ )	
	Dmol <sup>3</sup>	Gaussian-03	Dmol <sup>3</sup>	Gaussian-03	Dmol <sup>3</sup>	Gaussian-03
<b>1</b>	−2.975	−2.298	−5.088	−5.711	2.113	2.736
<b>2</b>	−3.132	−2.455	−5.199	−5.820	2.067	3.365
<b>3</b>	−3.709	−2.981	−5.598	−6.160	1.889	3.179
<b>4</b>	−3.610	−2.823	−5.455	−6.078	1.845	3.255
<b>5</b>	−3.836	−2.936	−5.556	−6.171	1.720	3.235
<b>6</b>	−4.069	−3.286	−5.969	−6.556	1.900	3.270
<b>7</b>	−2.784	−2.123	−4.806	−5.412	2.022	3.289
<b>8</b>	−2.943	−2.281	−4.920	−5.520	1.977	3.239
<b>9</b>	−3.537	−2.833	−5.274	−5.812	1.737	2.979

**Table 7**  
The electric dipole moment  $\mu$  (D) and the polarizability of nitriles **1–9**.

	<b>1</b>	<b>2</b>	<b>3</b>	<b>4</b>	<b>5</b>	<b>6</b>	<b>7</b>	<b>8</b>	<b>9</b>
$\mu_x$	0.75	2.48	7.57	0.26	1.18	6.86	2.76	4.68	10.13
$\mu_y$	−4.05	−3.81	−3.25	0.79	1.20	1.24	−5.54	−5.29	−4.71
$\mu_z$	−0.24	0.43	2.45	−1.01	0.31	1.56	0.37	1.07	3.16
$\mu_{rot}$	4.12	4.56	8.60	1.31	1.71	7.14	6.20	7.15	11.62
$\alpha_{xx}$	416.623	465.094	500.727	495.605	506.896	501.572	526.597	580.877	635.991
$\alpha_{xy}$	−52.756	−48.850	−49.745	7.803	−0.717	−62.478	−18.212	−25.863	−28.493
$\alpha_{yy}$	202.491	206.915	217.461	222.031	224.640	247.930	199.708	207.780	219.185
$\alpha_{xz}$	129.322	146.072	161.075	−9.067	−8.766	150.019	−2.501	−1.430	−1.216
$\alpha_{yz}$	−5.006	−3.056	−2.014	5.002	0.578	−2.408	2.947	3.341	3.375
$\alpha_{zz}$	106.762	117.741	125.129	69.741	76.855	130.800	74.737	79.052	78.991
$\langle \alpha \rangle$ (a.u.)	241.958	263.250	281.105	262.459	269.463	293.434	267.013	289.237	311.389
$10^{24} \times \alpha_{tot}$ (esu)	35.858	39.014	41.660	38.896	39.934	43.487	39.589	42.865	46.148

**Table 8**The hyperpolarizability of nitriles **1–9**.

	<b>1</b>	<b>2</b>	<b>3</b>	<b>4</b>	<b>5</b>	<b>6</b>	<b>7</b>	<b>8</b>	<b>9</b>
$\beta_{xxx}$	−296.527	528.785	−9986.423	5196.632	6126.237	−4137.768	−5499.648	−5424.822	−20983.499
$\beta_{xxy}$	124.206	251.305	−241.512	154.621	182.781	−669.606	−24.368	451.511	−1111.729
$\beta_{xyy}$	−32.365	−17.374	115.302	245.122	215.788	399.278	70.700	106.152	89.079
$\beta_{yyz}$	−15.496	−10.253	−2.842	−279.834	−267.568	−436.751	−40.240	−26.013	−20.819
$\beta_{xxz}$	−93.284	216.269	−3859.447	111.013	83.790	−1687.208	14.277	−23.647	41.456
$\beta_{xyz}$	29.709	89.203	−85.579	−43.191	−17.331	−252.984	−28.677	−30.040	5.509
$\beta_{yyz}$	−5.184	−4.065	51.840	31.950	55.008	194.976	−6.627	−5.226	6.809
$\beta_{xzz}$	−29.222	86.550	−1488.666	5.054	2.160	−678.206	36.328	34.105	49.085
$\beta_{yzz}$	−6.109	27.295	−31.783	−0.646	−6.876	−97.025	−32.805	−34.610	−36.815
$\beta_{zzz}$	−10.029	31.323	−575.059	−3.894	−5.776	−274.192	7.634	7.327	9.179
$\beta_{\text{tot}}$ (a.u)	388.001	699.195	12179.292	5450.036	6346.241	4906.687	5393.521	5299.179	20877.479
$10^{33} \times \beta_{\text{tot}}$ (esu)	3352.059	6040.553	105218.287	47084.494	54827.080	42390.344	46596.226	45781.193	180366.800

evaluated and compared to the experimental values obtained by EFISH and HRS measurement and several studies have been reported in literature [28–31].

The  $^1\text{H}$  and  $^{13}\text{C}$  chemical shifts were also determined theoretically by DFT method in the gaseous state as well as in  $\text{CDCl}_3$

[SCRF-PCM model] using the basis set B3LYP/6-311+G(2d,p) Giao. The shielding magnitude obtained from the computational calculations are converted into their corresponding chemical shifts using the conversion factor 182.4656 [ $^{13}\text{C}$ ] and 31.8821 [ $^1\text{H}$ ]. The experimental  $^{13}\text{C}$  chemical shifts are closer to the theoretical values and

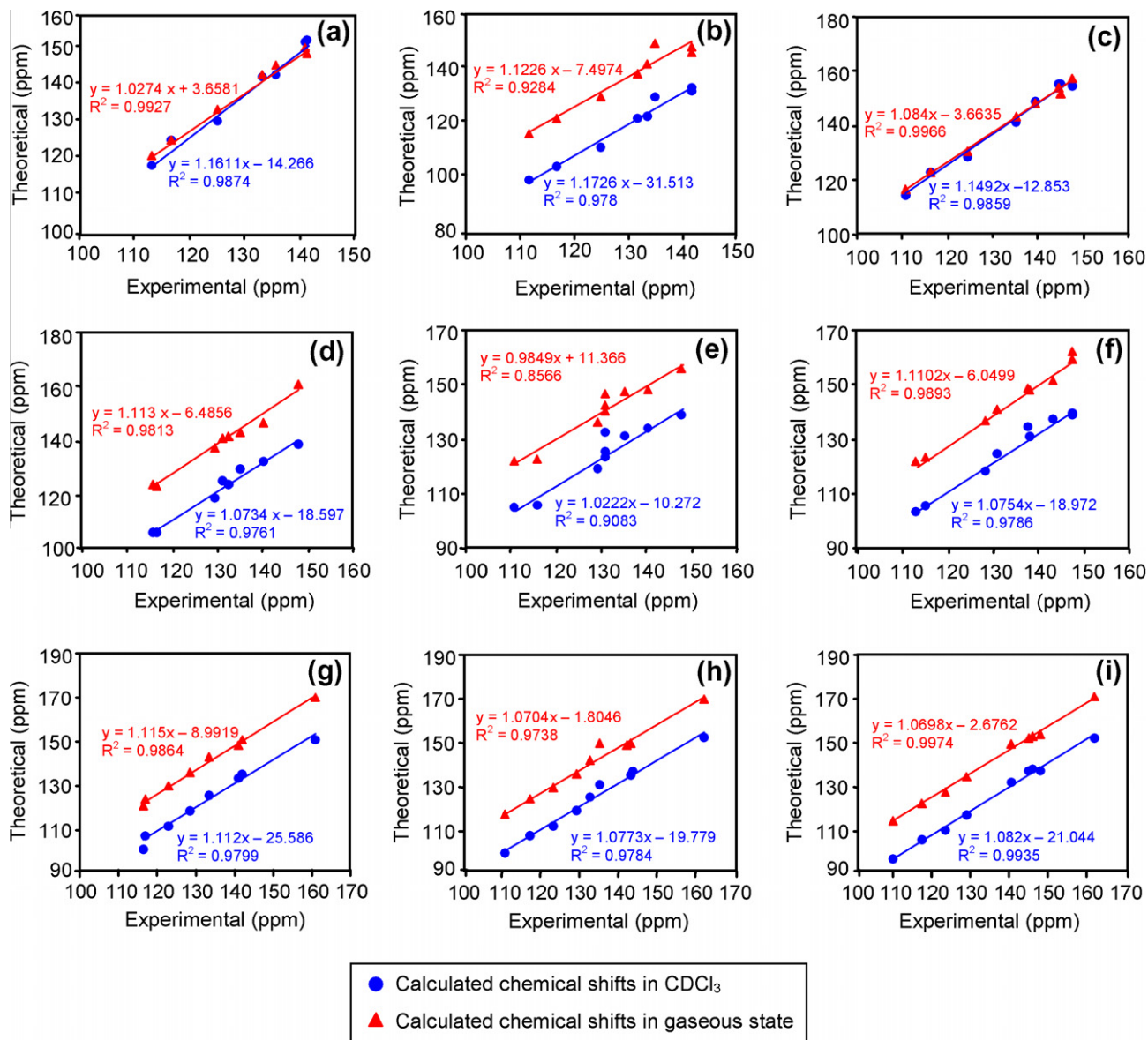


Fig. 5. (a-i). Correlation between the experimental and theoretical  $^{13}\text{C}$  chemical shifts for **1–9**.

**Table 9**Experimental and theoretical  $^1\text{H}$  NMR [SCRF-PCM model] spectral data (ppm) of nitriles **1–9** in  $\text{CDCl}_3$ .

Protons	<b>1</b>		<b>2</b>		<b>3</b>		<b>4</b>		<b>5</b>		<b>6</b>		<b>7</b>		<b>8</b>		<b>9</b>		
	Exp.	Theor.	Exp.	Theor.	Exp.	Theor.	Exp.	Theor.	Exp.	Theor.	Exp.	Theor.	Exp.	Theor.	Exp.	Theor.	Exp.	Theor.	
H(3)	7.45– 7.35	7.85 (7.92)	7.40– 7.33	7.82 (7.85)	7.63– 7.55	8.08 (8.80)	7.48	7.98 (8.07)	7.46	7.96 (7.70)	7.64	8.22 (8.14)	7.39	7.81 (8.14)	7.35	7.78 (7.60)	7.55	8.02 (7.49)	
H(4)	7.45– 7.35	7.80 (8.15)	7.40– 7.33	7.77 (8.10)	7.45– 7.40	7.83 (8.16)	7.37	7.82 (8.29)	7.35	7.79 (7.81)	7.39	7.80 (8.26)	7.27	7.58 (7.87)	7.23	7.55 (7.82)	7.29	7.61 (7.88)	
H(5)	7.03	7.35	7.03	7.38	7.16	7.57	7.55	8.23	7.57	8.26	7.71	8.44	6.97	7.29	6.97	7.32	7.12	7.73 (7.27)	
H(22)	7.64	8.03 (8.33)	7.54	7.97	7.79	8.14	7.65– (8.36)	8.08	7.59	8.02	7.84	8.21	7.61	7.99	7.52	7.93	7.76	8.09 (8.13)	
H(23)	7.45– 7.35	7.84 (7.76)	7.33– 7.40	7.71 (7.68)	8.29	8.78	7.41– (8.79)	7.87	7.42	7.75	8.32	8.82	7.41	7.83 (8.84)	7.36	7.69 (7.72)	8.27	8.72 (8.70)	
H(24)	7.45– 7.35	7.75 (7.64)	–	–	–	–	7.41– (7.44)	7.83	–	–	–	–	7.34	7.72 (7.55)	–	–	–	–	
H(25)	7.45– 7.35	7.80 (7.72)	7.33– 7.40	7.67 (7.76)	8.29	8.74	7.41– (8.80)	7.84	7.42	7.73	8.32	8.78	7.41	7.75	7.36	7.65 (7.52)	8.27	8.70 (8.68)	
H(26)	7.64	8.00 (8.05)	7.54	7.88 (7.94)	7.79	7.57	7.65– (8.02)	8.04	7.59	8.00 (8.16)	7.84	8.13	7.61	7.89	7.52	7.84 (7.78)	7.76	8.00 (7.84)	
H(52)	7.56	7.71	7.54	7.69	7.63– (8.44)	7.78	–	–	–	–	–	–	–	≈7.50	7.64	7.49 (8.27)	7.65 (8.23)	7.54	7.73 (8.27)
H(53)	7.45– 7.35	7.79 (7.81)	7.33– 7.40	7.81 (7.78)	7.45– (7.82)	7.86	8.01	8.71	8.02	8.70	8.07	8.74	≈6.91	7.09	6.91	7.10 (7.30)	6.94	7.14 (7.29)	
H(54)	7.45– 7.35	7.79 (7.71)	7.33– 7.40	7.84 (7.74)	7.45– (7.81)	7.89	7.41– (7.81)	7.89	7.51	7.92	7.56	7.99	–	–	–	–	–	–	
H(55)	7.45– 7.35	7.85 (7.68)	7.33– 7.40	7.83 (7.75)	7.45– (7.80)	7.89	7.65– (7.92)	8.14	7.67	8.14	7.73	8.18	≈6.91	7.33	6.91	7.34 (6.84)	6.94	7.37 (6.90)	
H(56)	7.56	8.34	7.54	8.27	7.63– (7.63)	8.39	7.83	8.16	7.83	8.15	7.84	8.17	≈7.50	8.20	7.49	8.19 (7.46)	7.54	8.24 (7.51)	

Values within parentheses are calculated values in gaseous state.

**Table 10**Experimental and theoretical  $^{13}\text{C}$  NMR [SCRF-PCM model] spectral data (ppm) of nitriles **1–9** in  $\text{CDCl}_3$ .

Carbons	<b>1</b>		<b>2</b>		<b>3</b>		<b>4</b>		<b>5</b>		<b>6</b>		<b>7</b>		<b>8</b>		<b>9</b>	
	Exp.	Theor.	Exp.	Theor.	Exp.	Theor.	Exp.	Theor.	Exp.	Theor.	Exp.	Theor.	Exp.	Theor.	Exp.	Theor.	Exp.	Theor.
C(3)	141.58	151.00	141.90	134.46	145.04	155.34	140.45	132.46	140.81	133.11	143.98	136.72	142.08	134.17	142.39	135.24	145.52	138.02
C(4)	125.19	129.00	124.87	112.43	124.63	128.43	129.73	118.33	129.42	118.02	128.90	117.66	123.15	110.48	122.87	110.12	122.56	109.90
C(5)	141.23	150.56	141.85	133.47	144.41	155.06	135.08	129.20	135.73	130.33	138.25	133.86	141.00	132.27	141.62	133.17	144.29	136.54
CCN	113.22	116.86	111.86	100.22	110.86	113.92	115.92	105.95	111.24	104.32	113.56	102.88	116.65	99.61	110.33	97.89	109.16	96.67
CN	116.95	123.55	116.92	105.55	116.09	122.67	116.51	105.41	116.21	105.07	115.66	104.54	117.23	106.26	116.90	105.91	116.43	105.42
C(21)	133.28	140.90	131.73	123.50	139.44	148.67	132.67	123.41	131.22	122.69	138.74	130.40	133.47	124.65	131.99	123.86	139.70	132.12
C(51)	135.79	141.63	133.56	124.17	135.24	140.98	131.29	124.73	131.22	124.77	131.59	124.29	128.61	117.54	128.43	117.32	128.07	117.05
C(52)	–	–	–	–	–	–	–	–	148.05	138.52	148.07	138.45	148.13	138.76	–	–	–	–
C(54)	–	–	–	–	–	–	–	–	–	–	–	–	160.88	150.31	161.01	150.58	161.56	151.82
C(24)	–	–	135.01	130.87	147.68	154.16	–	–	131.22	131.99	148.13	138.04	–	–	134.65	130.13	147.33	137.82
			(151.75)	(157.18)					(151.52)		(158.44)				(169.32)	(169.54)	(170.52)	(153.79)

Values within parentheses are calculated values in gaseous state.

the data are displayed in Table 10. The correlation between experimental and theoretical  $^{13}\text{C}$  values of side chain carbons and *ipso* carbons are indicated in Fig. 5(a–i). However, theoretically determined  $^1\text{H}$  chemical shifts are generally higher when compared to experimental values and large deviations are observed in the nitriles **4–6** containing *o*-nitrophenyl ring at C-5 and the data are displayed in Table 9.

NBO analyses at two levels of calculations [B3LYP/6-31G(d) and B3LYP/6-311+G(d,p)] were carried out for the nitriles **1–9**

and the important second order perturbative estimates of donor–acceptor interactions are displayed in Table 11. The occupancies and the energies of the orbitals involved in primary delocalization are reported in Table 12. The labelling of atoms followed in the NBO analysis are indicated in Fig. 6. The presence of cyano group is expected to cause delocalization of electrons from C5–C4 bond to C3–C2 bond instead of C5–C4 bond to C52–C51/C56–C51 bonds and this expectation is supported by the delocalization

**Table 11**NBO analysis of nitriles **1–9** by DFT method [B3LYP/6-311+G(d,p)].

Donor NBO BD(2)	Acceptor NBO BD*(2)/LP	<b>1</b>	<b>2</b>	<b>3</b>	<b>4</b>	<b>5</b>	<b>6</b>	<b>7</b>	<b>8</b>	<b>9</b>
C5–C4	C52–C51/C56– C51*	13.08 (13.34)	12.98 (13.16)	12.62 (13.02)	11.24 (15.30)	11.10 (10.91*)	10.70 (12.53*)	12.74 (12.58)	12.68 (12.92)	12.57 (13.11)
C5–C4	C3–C2	20.03 (21.18)	20.46 (21.72)	21.89 (22.95)	19.11 (20.09)	19.43 (19.45)	20.48 (21.63)	20.89 (20.66)	21.26 (21.52)	22.66 (23.66)
C56–C55	C54–C53	20.13 (20.08)	20.17 (20.18)	20.29 (20.36)	18.07	—	—	21.35 (21.21)	21.32 (21.36)	21.41 (21.27)
C56–C55	C52–C51	19.62 (19.14)	19.59 (19.18)	19.16 (19.07)	20.45	—	—	16.31 (16.13)	16.28 (16.73)	16.13 (16.31)
C54–C53	C56–C55	19.02 (19.24)	18.92 (19.19)	18.79 (18.93)	19.68	—	—	14.99 (15.26)	14.92 (15.52)	14.64 (15.11)
C54–C53	C52–C51	20.82 (21.05)	20.98 (21.27)	21.39 (21.75)	19.65	—	—	22.77 (22.78)	23.00 (22.48)	23.58 (23.12)
C52–C51	C56–C55	18.20 (18.70)	18.17 (18.74)	18.52 (18.65)	15.80	—	—	19.51 (19.71)	19.46 (19.78)	19.37 (19.35)
C52–C51	C54–C53	20.11 (20.28)	19.94 (20.10)	19.53 (19.67)	20.47	—	—	18.09 (18.01)	17.98 (18.73)	17.80 (18.56)
C52–C51/C56– C51*	C5–C4	16.80 (17.49)	17.04 (17.88)	18.52 (18.49)	10.42 (11.94)	10.48 (10.54*)	10.68 (12.56*)	18.34 (18.05)	18.61 (18.72)	19.39 (19.89)
C3–C2	C5–C4	13.43 (14.27)	13.24 (13.92)	12.49 (13.49)	13.31 (14.22)	13.11 (13.18)	12.50 (13.74)	13.09 (13.30)	12.97 (13.56)	12.52 (13.60)
C3–C2	C1–N6	18.83 (19.41)	18.88 (19.52)	18.88 (19.44)	18.28 (18.53)	18.33 (18.24)	18.49 (19.01)	19.13 (18.99)	19.19 (19.44)	19.24 (19.81)
C3–C2	C22–C21	12.26 (14.05)	12.65 (14.43)	14.23 (15.90)	11.95 (13.43)	12.32 (12.20)	13.82 (15.24)	12.49 (12.32)	12.91 (13.14)	14.74 (16.33)
C22–C21	C3–C2	13.51 (15.75)	13.52 (15.34)	12.89 (14.48)	—	13.92 (13.82)	13.18 (14.75)	— (13.43)	13.43 (13.73)	12.94 (14.48)
C22–C21	C23–C24	20.13 (20.24)	22.09 (22.91)	23.92 (24.42)	19.71 (19.46)	21.75 (21.97)	23.37 (23.77)	20.32 (20.35)	22.32 (23.19)	24.24 (24.80)
C22–C21	C25–C26	19.25 (19.26)	19.82 (19.78)	17.16 (17.21)	19.14 (18.86)	19.71 (19.73)	17.23 (17.29)	19.23 (19.36)	19.82 (20.11)	17.05 (17.11)
C23–C24	C22–C21	20.62 (20.92)	18.79 (18.63)	17.73 (17.90)	21.02 (21.12)	19.15 (19.25)	17.99 (18.17)	20.48 (20.58)	18.61 (18.53)	17.58 (17.80)
C23–C24	C25–C26	20.22 (20.34)	19.22 (19.58)	20.72 (20.86)	19.92 (19.65)	18.93 (19.08)	20.54 (20.63)	20.36 (20.39)	19.35 (19.89)	20.78 (20.91)
C25–C26	C22–C21	19.57 (19.21)	18.71 (18.53)	20.79 (20.26)	19.61 (18.84)	18.75 (18.60)	20.88 (20.41)	19.56 (19.36)	18.74 (19.02)	20.71 (20.15)
C25–C26	C23–C24	19.46 (19.29)	19.86 (19.59)	18.73 (18.43)	19.75 (19.34)	20.13 (19.90)	19.07 (18.94)	19.35 (19.32)	19.77 (19.88)	18.51 (18.22)
C56–C51	C55–C54	—	—	—	21.59	21.46 (21.35)	21.00 (21.00)	—	—	—
C56–C51	C53–C52	—	—	—	19.37	19.36 (19.25)	19.35 (19.33)	—	—	—
C55–C54	C56–C51	—	—	—	20.32	20.38 (20.48)	20.58 (21.47)	—	—	—
C55–C54	C53–C52	—	—	—	24.40	24.30 (24.18)	24.01 (24.13)	—	—	—
C53–C52	C56–C51	—	—	—	20.41	20.41 (20.25)	20.37 (19.64)	—	—	—
C53–C52	C55–C54	—	—	—	17.07	17.05 (17.15)	17.05 (17.27)	—	—	—
C53–C52	N10–O12	—	—	—	25.20	25.09 (24.41)	24.70 (24.53)	—	—	—
N10–O12	LP(3) O11	—	—	—	12.21 (12.35)	12.22 (12.49)	12.22 (13.61)	—	—	—
C23–C24	N7–O9	—	—	26.24 (28.24)	—	—	25.59 (27.05)	—	—	26.67 (28.72)
N7–O9	LP(3) O8	—	—	12.12 (12.74)	—	—	12.23 (12.89)	—	—	12.05 (12.66)
LP	BD*/RY*	—	—	—	—	—	—	—	—	—
LP(1)N6	RY*(1) Cl	17.41 (16.84)	17.36 (16.79)	17.59 (16.74)	17.58 (16.87)	17.56 (17.11)	17.53 (16.75)	17.46 (17.17)	17.66 (17.07)	17.66 (16.75)
LP(1)N6	BD*(1) C2–C1	11.38 (12.02)	11.39 (12.05)	11.39 (12.12)	11.48 (12.67)	11.47 (12.61)	11.48 (12.14)	11.43 (12.53)	11.35 (11.95)	11.31 (12.11)
LP(3)O8	BD*(2)N7–O9	—	—	160.85 (179.85)	—	—	161.51 (181.14)	—	—	160.22 (179.18)
LP(2)O9	BD*(1)C24–N7	—	—	11.87 (11.83)	—	—	11.70 (12.11)	—	—	11.48 (11.74)
LP(2)O9	BD*(1)N7–O8	—	—	18.84 (19.12)	—	—	18.83 (19.10)	—	—	18.84 (19.09)
LP(2)O8	BD*(1)C24–N7	—	—	11.52 (11.76)	—	—	11.66 (12.03)	—	—	11.43 (11.66)
LP(2)O8	BD*(1)N7–O9	—	—	18.77 (19.02)	—	—	18.77 (19.04)	—	—	18.77 (18.99)

(continued on next page)

**Table 11** (continued)

Donor NBO BD(2)	Acceptor NBO BD*(2)/LP	1	2	3	4	5	6	7	8	9
LP(2)O12	BD*(1)C52–N10				11.97 (12.04)	12.01 (12.91)	12.12 (12.40)			
LP(2)O11	BD*(1) C52– N10				10.90 (11.32)	10.91 (11.89)	10.90 (11.51)			
LP(2)O11	BD*(1)N10–O12				18.99 (18.49)	18.98 (19.34)	18.95 (19.04)			
LP(3)O11	BD*(2)N10–O12				155.25 (155.67)	155.05 (159.28)	154.46 (172.88)			
LP(2)O12	BD*(1) N10– O11				18.71 (18.47)	18.73 (19.24)	18.79 (19.28)			
LP(2)O13	BD*(2)C54–C53							31.16 (32.22)	31.40 (33.29)	32.00 (32.41)
LP(3)Cl 7	BD*(2)C23–C24		12.58 (12.11)			12.80 (12.42)			12.44 (12.36)	
LP(3)O11	BD*(1)N10–O11						10.67			

Values within parentheses are calculated values according to the basis set B3LYP/6-31G(d).

**Table 12**

Energies, occupancies of primary donor and acceptor orbitals and their delocalization energies in nitriles **1–9** by DFT method [B3LYP/6-311+G(d,p)].

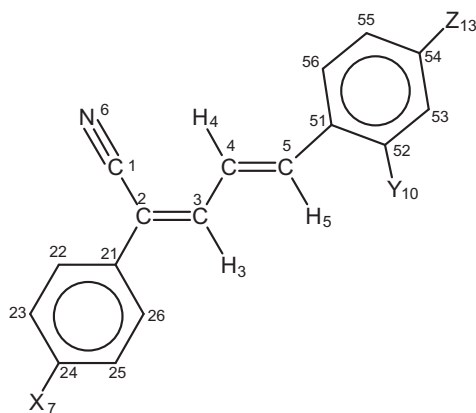
Nitriles	Donor NBO	Occupancy	Energy (a.u)	Acceptor NBO	Occupancy	Energy (a.u)	$E_2$ (kcal mol <sup>-1</sup> )
1	BD(2) C54–C53/BD(2) C5–C4 (1.80293)	1.65235 (1.80293)	−0.26202 (−0.27198)	(BD*(2) C52–C51 (BD*(2) C3–C2)) (0.23634)	0.38516 (0.39017)	0.01609 (0.01648) (−0.00417)	20.82 (21.18) 22.09 (22.91)
2	BD(2) C22–C21	1.62337 (1.62056)	−0.26793 (−0.26098)	BD*(2) C23–C24	0.38917 (0.63206)	−0.00236 (−0.15225)	160.85 (179.85)
3	LP(3)O8	1.45207 (1.43744)	−0.2912 (−0.28142)	BD*(2) N7–O9	0.63206 (0.65804)	(−0.16372)	
4	LP(3)O11	1.44655 (1.43553)	−0.30016 (−0.28300)	BD*(2) N10–O12	0.62360 (0.61790)	−0.15150 (−0.13649)	155.25 (155.67)
5	LP(3)O11	1.44667 (1.44166)	−0.30266 (−0.28492)	BD*(2) N10–O12	0.62253 (0.62260)	−0.15376 (−0.13543)	155.05 (159.28)
6	LP(3)O8	1.44626 (1.43366)	−0.30913 (−0.28668)	BD*(2) N7–O9	0.61950 (0.65399)	−0.15953 (−0.16853)	154.46 (181.14)
7	LP(2)O13	1.83058 (1.82817)	−0.33037 (−0.31556)	BD*(2) C54–C53	0.38977 (0.39308)	0.00923 (0.02196)	31.16 (32.22)
8	LP(2)O13	1.82903 (1.82697)	−0.33264 (−0.32045)	BD*(2) C54–C53	0.38891 (0.39991)	0.00654 (0.00637)	31.40 (33.29)
9	LP(3)O8	1.45430 (1.43950)	−0.28858 (−0.27788)	BD*(2) N7–O9	0.63418 (0.66048)	−0.14878 (−0.16044)	160.22 (179.18)

Values within parentheses are calculated values according to the basis set B3LYP/6-31G(d).

energies in **Table 11**. Moreover, the introduction of substituents in the phenyl ring attached to C2 carbon (cyanomethylene carbon) enhances this delocalization energy whereas the introduction of nitro group in the cinnamylidene (phenyl ring attached to C5 carbon) ring lowers this delocalization energy. The delocalization energies corresponding to the transfer of electrons from C3–C2 bond to C1–N6 bond also support this conclusion. The energy corresponding to the delocalization of electrons from C52–C51/C56–C51 bond to C5–C4 bond is increased by the presence of substituents attached to the phenyl ring at C-2 and by the methoxy substituent attached to the *para* position of phenyl ring at C-5. However, the presence of *ortho* nitro group in the phenyl ring at C-5 lowers this delocalization energy. This is due to the tilting of *o*-nitrophenyl ring from the plane of the side chain moiety. The introduction of substituents in the phenyl rings attached to C2 and C5 carbons decreases the delocalization of electrons from C22–C21 bond to C3–C2 bond.

From **Table 12**, it is seen that in nitro derivatives primary delocalization occurs within the orbitals of the nitro group attached to the *para* position of the phenyl ring at C-2 (**3**, **6** and **9**) and *ortho* position of the phenyl ring at C-5 (**4** and **5**). In nitro derivatives **3**, **6** and **9** the lone pair of electrons available on oxygen (O8) is

delocalized onto the antibonding orbitals of N7–O9 bond. Comparison of delocalization energies of nitriles **6** and **9** with that of **3** reveals that the introduction of electron releasing methoxy substituent at the *para* position of phenyl ring attached to C5 carbon lowers this delocalization energy whereas the electron withdrawing nitro substituent at the *ortho* position of the phenyl ring attached to C5 carbon enhances this delocalization energy. In *ortho* nitro derivatives **4** and **5** primary delocalization occurs from the lone pair of electrons available on oxygen atom (O11) to the antibonding orbital of N10–O12 bond and this delocalization is enhanced by the presence of chloro substituent at the *para* position of phenyl ring at C-2 [ $E_2(5) > E_2(4)$ ]. In methoxy derivatives **7** and **8** delocalization occurs from the lone pair of electrons available on oxygen atom of the methoxy group (O13) to the nearby antibonding orbital of C54–C53 bond and this delocalization energy is higher for *p*-chloro derivative **8** compared to unsubstituted derivative **7**. In nitrile **1** without ring substituent primary delocalization occurs from the bonding orbital of C(54)–C(53) to antibonding orbital of C(52)–C(51) according to higher basis set and from the bonding orbital of C(5)–C(4) to antibonding orbital of C(3)–C(2) (with the lower basis set). In *p*-chloro derivative **2** primary delocalization occurs within the orbitals of *p*-chlorophenyl ring and the



X	Y	Z
1; H	H	H
2; Cl(7)	H	H
3; N(7)	H	H
4; H	N(10)	H
5; Cl(7)	N(10)	H
6; N(7)	N(10)	H
7; H	H	O(13)-CH <sub>3</sub> (14)
8; Cl(7)	H	O(13)-CH <sub>3</sub> (14)
9; N(7)	H	O(13)-CH <sub>3</sub> (14)

**Fig. 6.** Labelling of atoms in **1–9**.

bonding pair of electrons in C22–C21 bond is delocalized onto the antibonding orbital of C24–C23 bond.

### 3.2. Analysis of chemical shifts

The chemical shifts of *p*-chlorophenyl derivatives **2**, **5** and **8** and *p*-nitrophenyl derivatives **3**, **6** and **9** have been compared with those of **1**, **4** and **7**. Such comparison reveals that there is no appreciable change in the chemical shifts of the side chain protons H(3), H(4) and H(5) and the side chain carbons C(3), C(4) and C(5) by the introduction of chloro group at the *para* position of the phenyl ring at C-2. However, the introduction of nitro substituent in the *para* position of phenyl ring at C-2 slightly deshields the H(3) and H(5) protons and C(3) and C(5) carbons due to electron withdrawing nature of nitro group.

Comparison of the chemical shifts of side chain protons H(3), H(4) and H(5) in **1** and **4** reveals that the introduction of the nitro substituent at the *ortho* position of the cinnamylidene moiety causes no change in the chemical shifts of H(3) and H(4) protons but deshields H(5) proton appreciably (+0.52 ppm). Similar deshielding magnitude has also been observed in **5** (+0.54 ppm) and **6** (+0.55 ppm) due to the presence of nitro substituent at the *ortho* position of the phenyl ring of the cinnamylidene moiety (i.e., phenyl ring at C-5). The introduction of the nitro substituent at the *ortho* position of phenyl ring in cinnamylidene moiety shields

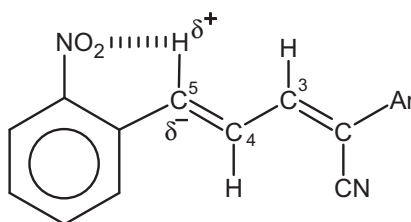


**Fig. 7.** Steric polarization interaction in nitro derivatives.

C(3) and C(5) carbons but deshields C(4) carbon. The shielding magnitude observed on C(5) is considerably higher ( $-6.15\text{ ppm}$ ) than that on C(3) ( $-1.13\text{ ppm}$ ). Such large deshielding magnitude observed on H(5) proton and shielding magnitude observed on C(5) suggest that the nitro group must be *syn* to the H(5) proton in **4–6** as shown in Fig. 7. In this orientation, the nitro group experiences severe steric interaction with H(5) proton. As a result of this interaction C(5)-H bond is polarized and the H(5) proton acquires a slight positive charge and corresponding carbon acquires a slight negative charge.

In order to find out the influence of the methoxy substituent on the side chain protons and the side carbons, the chemical shifts of **1–3** have been compared with those of **7–9**. There is no appreciable change in the chemical shifts H(3) and H(5) protons and C(3) and C(5) carbons by the introduction of methoxy substituent at the *para* position of the phenyl ring at C-5 in **1–3**. However, H(4) protons and C(4) carbons are found to be slightly shielded due to the introduction of methoxy substituent at *para* position of the phenyl ring at C-5. The mesomeric interaction of the electron releasing methoxy substituent places a small amount of negative charge on C(4) carbon and this negative charge is transmitted to the corresponding hydrogen and hence H(4) protons and C(4) carbons are shielded due to the presence of methoxy substituent in **7–9**.

#### 4 Conclusion

2,5-Diaryl penta-2,4-dienenitriles **1–9** were synthesized and characterized by spectral studies. From the coupling constants, chemical shifts and computational calculations the favored conformation is predicted to be the one in which all side chain protons are *trans* to each other and H(3) proton is *trans* to CN group. Further, *syn* orientation of NO<sub>2</sub> group with respect to H(5) proton in **4–6** is revealed by computational calculations and chemical shifts. HOMO–LUMO energies, dipole moment, polarizabilities and first order hyperpolarizabilities were determined theoretically. The highest  $\beta_{\text{tot}}$  is observed for the nitrile **9** hence it is the best NLO candidate among the nitriles **1–9**. The <sup>1</sup>H and <sup>13</sup>C chemical shifts were also determined theoretically by DFT method and they are in agreement with the experimental values. NBO analysis were carried out and analyzed. The effect of introduction of substituents in the phenyl ring on the chemical shifts of the side chain protons and their carbons were analyzed in detail.

### **Acknowledgement**

The authors thank the NMR Research Centre, Indian Institute of Science, Bangalore for recording the NMR spectra.

## Appendix A. Supplementary material

Mass fragmentation schemes (Schemes S1 and S2) and the corresponding table (Table S1) for the nitriles 1–9 are provided. Sup-

plementary data associated with this article can be found, in the online version, at doi:10.1016/j.molstruc.2011.03.060.

## References

- [1] P.N. Prasad, D.J. Williams, Non-linear Optical Effects in Molecules and Polymers, Wiley, New York, 1991.
- [2] S. Manivannan, S.K. Tiwari, S. Dhanuskodi, Solid State Commun. 132 (2004) 123–127.
- [3] K. Kobayashi, Non-linear Optics of Organics and Semiconductors, Springer Verlag, Tokyo, 1989.
- [4] K. Bhat, K.J. Chang, M.D. Aggarwal, W.S. Wang, B.G. Penn, D.O. Frazier, Mater. Chem. Phys. 44 (1996) 261–266.
- [5] A. Karakas, A. Elmali, H. Unver, I. Svoboda, J. Mol. Struct. 702 (2004) 103–110.
- [6] H. Unver, A. Karakas, A. Elmali, J. Mol. Struct. 702 (2004) 49–54.
- [7] J.O. Morley, J. Chem. Soc. Perkin Trans. 2 (1995) 731–734.
- [8] A. Ali, M. Bliese, J.A.M. Rasmussen, R.M. Sargent, S. Saubermann, D.G. Sawutz, J.S. Wilkie, D.A. Winkler, K.N. Winzenberg, R.C.J. Woodgate, Bioorg. Med. Chem. Lett. 17 (2007) 993–997.
- [9] F. Saczewski, A. Stencel, A.M. Bienczak, K.A. Langowska, M. Michaelis, W. Werel, R. Halasa, P. Reszka, P.J. Bednarski, Eur. J. Med. Chem. 43 (2008) 1847–1857.
- [10] M. Hranjec, G. Pavlovic, M. Marjanovic, M. Kralj, G. Karminski-Zamola, Eur. J. Med. Chem. 45 (2010) 2405–2417.
- [11] M. Hranjec, G. Karminski-Zamola, Molecules 12 (2007) 1817–1828.
- [12] F. Fringuelli, G. Pani, O. Piermattei, F. Pizzo, Tetrahedron 50 (1994) 11499–11508.
- [13] (a) G.D. Diana, D. Cutcliffe, D.L. Volkots, J.P. Mallamo, T.R. Bailey, N. Vescio, R.C. Oglesby, T.J. Nitz, J. Wetzel, V. Girandu, D.C. Pevear, F.J. Dutko, J. Med. Chem. 36 (1993) 3240–3250;  
 (b) M.E. Fabiani, Drug News Perspect. 12 (1999) 207–215;  
 (c) M. Chihiro, H. Nagamoto, I. Takemura, K. Kitano, H. Komatsu, K. Sekiguchi, F. Tabusa, T. Mori, M. Tominaga, Y. Yabuuchi, J. Med. Chem. 38 (1995) 353–358;  
 (d) I.K. Khanna, R.M. Weier, Y. Yu, X.D. Xu, I.K. Khanna, R.M. Weier, Y. Yu, X.D. Xu, F.J. Koszyk, P.W. Callins, C.M. Koboldt, A.W. Veenhuizen, W.E. Perkins, J.J. Casler, J.L. Masferrer, Y.Y. Zhung, S.A. Gregory, K. Seibert, C.P. Isakson, J. Med. Chem. 40 (1997) 1634–1647.
- [14] (a) M.A. Cohen, J. Sawden, N.J. Turner, Tetrahedron Lett. 31 (1990) 7223–7226;  
 (b) J. Crossby, J. Moiller, J.S. Parratt, N.J. Turner, J. Chem. Soc. Perkin Trans. 1 (1994) 1679–1687;  
 (c) F.T. Luo, A. Jeevanandam, Tetrahedron Lett. 39 (1998) 9455–9456.
- [15] S. Muruyama, X.-T. Tao, H. Hokari, T. Noh, Y. Zhang, T. Wada, H. Sasabe, H. Suzuki, T. Watanabe, S. Miyata, Chem. Lett. (1998) 749–750.
- [16] (a) J.L. Segura, N. Martin, M. Hanack, Eur. J. Org. Chem. (1999) 643–651;  
 (b) R. Gomez, J.L. Segura, N. Martin, Chem. Commun. (1999) 619–620.
- [17] H.C. Yeh, S.J. Yeh, C.T. Chen, Chem. Commun. (2003) 2632–2633.
- [18] Y. Yue, J. Kang, M. Yu, Dyes Pigments 83 (2009) 72–80.
- [19] C.C. Silveira, G. Perin, A.L. Braga, M.J. Dabdoub, R.G. Jacob, Tetrahedron 57 (2001) 5953–5959.
- [20] (a) B. Delley, J. Chem. Phys. 92 (1990) 508–517;  
 (b) B. Delley, J. Chem. Phys. 113 (2000) 7756–7764;  
 (c) A.D. Becke, Phys. Rev. A 38 (1988) 3098–3100;  
 (d) C. Lee, W. Yang, R.G. Parr, Phys. Rev. B 37 (1988) 785–789.
- [21] M.J. Frisch, G.W. Trucks, H.B. Schlegel, G.E. Scuseria, M.A. Robb, J.R. Cheeseman, V.G. Zakrzewski, J.A. Montgomery Jr., R.E. Stratmann, J.C. Burant, S. Dapprich, J.M. Millam, A.D. Daniels, K.N. Kudin, M.C. Strain, O. Farkas, J. Tomasi, V. Barone, M. Cossi, R. Cammi, B. Mennucci, C. Pomelli, C. Adamo, S. Clifford, J. Ochterski, G.A. Peterson, P.Y. Ayala, Q. Cui, K. Morokuma, P. Salvador, J.J. Dannenberg, D.K. Malick, A.D. Rabuck, K. Raghavachari, J.B. Polesman, J. Cioslowski, J.N. Ortiz, A.G. Baboul, B.B. Stefanov, G. Liu, A. Liashenko, P. Piskorz, I. Komaromi, R. Gomperts, R.L. Martin, D.J. Fox, T. Keeth, M.A. Allalham, C.Y. Peng, A. Nanayakkara, M.W. Wong, J.L. Anders, C. Gonzales, M. Challacombe, P.M. Gill, B. Johnson, W. Chen, M. Head-Gordon, E.S. Replogle, J.A. Peple, Gaussian 98, Revision A. 9, Pittsburg, Pa: Gaussian IC, 2001.
- [22] A. Loupy, M. Pellet, A. Petit, G. Vo-Thanh, Org. Biomol. Chem. 3 (2005) 1534–1540.
- [23] I. Esen, C. Yolacan, F. Aydogan, Bull. Korean Chem. Soc. 31 (2010) 2289–2292.
- [24] M.J. Percino, V.M. Chapela, L.F. Montiel, E. Perez-Gutierrez, J.S. Maldonado, Chem. Papers 64 (2010) 360–367.
- [25] R. Archana, A. Balamurugan, A. Manimekalai, A. Thiruvalluvar, R.J. Butcher, Acta Crystallogr. E 65 (2009) o2953.
- [26] A. Karakas, A. Elmali, H. Unver, I. Svoboda, Spectrochim. Acta A 61 (2005) 2979–2987.
- [27] I. Sheikholesla, M. Hosseini, Mashhadizadeh, S. Saeid-Nia, J. Coord. Chem. 57 (2004) 417–423.
- [28] M.G. Papadopoulos, A.J. Sadlej, J. Leszczynski, Non-linear Optical Properties of Matter, from Molecules to Condensed Phases, Springer, The Netherlands, 2006.
- [29] E. Hendrickx, K. Clays, A. Persoons, C. Dehu, J.L. Bredas, J. Am. Chem. Soc. 117 (1995) 3547–3555.
- [30] P.C. Ray, Chem. Phys. Lett. 394 (2004) 354–360.
- [31] P.C. Ray, J. Leszczynski, Chem. Phys. Lett. 399 (2004) 162–166.